



Heterogeneous formation and light absorption of secondary organic aerosols from acetone photochemical reactions: remarkably enhancing effects of seeds and ammonia

Si Zhang¹, Yining Gao¹, Xinbei Xu¹, Luyao Chen¹, Can Wu^{1,2}, Zheng Li¹, Rongjie Li¹, Binyu Xiao¹, Xiaodi Liu¹, Rui Li^{1,2}, Fan Zhang^{1,2}, and Gehui Wang^{1,2}

¹Key Lab of Geographic Information Science of the Ministry of Education, School of Geographic Sciences, East China Normal University, Shanghai 200241, China

²Institute of Eco-Chongming, 20 Cuiniao Rd., Chongming, Shanghai 202150, China

Correspondence: Gehui Wang (ghwang@geo.ecnu.edu.cn)

Received: 9 July 2024 – Discussion started: 18 July 2024

Revised: 4 November 2024 – Accepted: 4 November 2024 – Published: 19 December 2024

Abstract. Secondary organic aerosols (SOAs) from highly volatile organic compounds (VOCs) are currently not well represented in numerical models as their heterogeneous formation mechanisms in the atmosphere remain unclear. Based on the smog chamber experiments, here we investigated the yield and formation pathway of SOA from acetone photochemical reactions under low-NO_x conditions in the presence of preexisting haze particles ((NH₄)₂SO₄ and NH₄HSO₄) and saline mineral particles (Na₂SO₄) under ammonia-rich conditions. Our results showed that the yield of acetone-derived SOA is remarkably enhanced via multiphase reactions in the presence of these preexisting seeds, especially for the saline mineral particles. We found that aerosol acidity is a key factor controlling the formation pathways of acetone-derived SOA, in which organic acids, alcohol, and carbonyls produced from acetone photochemical reactions dissolve into the aqueous phase of the preexisting seeds and subsequently esterify and/or oligomerize into SOAs that consist of larger molecules on the acidic aerosols but smaller molecules on the neutral mineral aerosols. Moreover, the light absorption ability of the acetone-derived SOA formed on (NH₄)₂SO₄ aerosols is stronger than that formed on Na₂SO₄ mineral particles, especially in the presence of ammonia, due to a formation of N-containing organics. Through comparison with that from methylglyoxal (MGly), we found that the total SOA from acetone in the chamber is 2.8–8.2 times that from the irreversible uptake of MGly, suggesting that only considering MGly as the precursor of acetone-derived SOA will probably underestimate the role of acetone in global SOA production since acetone abundantly exists in the troposphere.

1 Introduction

Secondary organic aerosols (SOAs) are the major component of fine particles in the atmosphere and produced from the photochemical oxidation of volatile organic compounds (VOCs) (R. Zhang et al., 2015; Srivastava et al., 2022; G. Wang et al., 2016), which significantly affects human health and global climate change (Jo et al., 2023; Chowdhury et al., 2022). However, current numeric models cannot

predict the evolution of atmospheric SOA accurately; one of the reasons is that models often only consider the partitioning process of condensable oxidation products of VOCs as the major formation pathway of SOA and neglect the contribution of heterogeneous reactions of highly volatile organic compounds to atmospheric SOA (Heald et al., 2005; Li et al., 2023).

A number of researchers have reported that SOA formation can be promoted significantly in the presence of hy-

drated seeds by heterogeneous reactions (Wong et al., 2015; Nguyen et al., 2014; Liu et al., 2018; Ge et al., 2017). For instance, Wong et al. (2015) reported that more isoprene SOA was formed on deliquescent ammonium sulfate seeds in comparison with that on the efflorescent ones. Such an enhancing effect of multiphase chemistry on SOA formation has also been found by Liu et al. (2018) and Wang et al. (2022) in their laboratory experiments. Their results showed that SOA multiphase formation is affected by the aerosol liquid phase properties such as acidity, ionic strength, and mixing state, which can alter the gas-to-particle phase partitioning of VOCs and change the formation process of SOA (Zhang et al., 2023; Riva et al., 2016, 2019; Bateman et al., 2014; Kampf et al., 2013; Wei et al., 2022). Amorim et al. (2020) analyzed the OH reactivities of organic acids in aqueous phases with different pH and found that all the organic acids exhibited larger OH reactivities under basic conditions than those under acidic conditions, indicating that aerosol acidity can influence the gas-particle partitioning and the multi-generation oxidation of volatile organics in liquid phase (Wei et al., 2022; Amorim et al., 2020, 2021; Zhao et al., 2006; Lv et al., 2022). Moreover, a few studies reported that the uptake of VOC oxidation products by inorganic aerosols can be affected by a salting-in/salting-out effect (Waxman et al., 2015; C. Wang et al., 2016). These results suggest that heterogeneous reactions of VOCs are important sources of atmospheric SOA, which are complex and affected by many factors. Currently, only a limited number of volatile organics, such as glyoxal, methylglyoxal (MGly), formaldehyde, and epoxydiols, have been investigated by chemical transport models for their contribution to the atmospheric SOA through heterogeneous reactions (Heald et al., 2005; Li et al., 2023; Fu et al., 2008; Moch et al., 2020), while the role of heterogeneous reactions in SOA formation from many other more volatile organics in the atmosphere is still unclear and is ignored generally by model work.

Compared to glyoxal, MGly, and formaldehyde, acetone is much more volatile, which is of a Henry's law constant (K_H) 2–4 orders of magnitude lower than the three species and abundantly exists in the atmosphere from the ground surface to the upper troposphere (Seinfeld and Pandis, 2006). Acetone can be directly emitted from the natural and anthropogenic sources and indirectly produced from oxidation of hydrocarbons (Jacob et al., 2002; Wang et al., 2023). Photolysis and OH oxidation are main sinks of acetone in the atmosphere, with photolysis contributing 45 % of the sink, OH oxidation 30 %, and ocean uptake and dry deposition to land 25 % (Jacob et al., 2002). Numerous studies have reported the reaction mechanisms of acetone's photolysis and OH oxidation, and have estimated their contributions to hydroxyl radicals in the upper troposphere and lower stratosphere, respectively (Stefan and Bolton, 1999; Arnold et al., 2004; Raff et al., 2005; Wang et al., 2020). However, the role of acetone in SOA heterogeneous formation remains unclear. A laboratory experiment showed that deliquesced inorganic aerosols

may promote SOA formation from the photochemical oxidation of acetone significantly (Ge et al., 2017), but up to now the yield of SOA derived from acetone photochemical reactions and the impact of inorganic aerosol physicochemical properties on SOA formation from acetone have not been reported. Therefore, the formation mechanism and the importance of acetone-derived SOA in the atmosphere remain unclear, where acetone ubiquitously co-exists with NH_3 and preexisting aerosols. MGly is an important product of acetone photochemical reactions, with 14 % molar yield as calculated by GEOS-Chem, which can partition into the aqueous phase followed by oligomerization, oxidation by OH, and/or reaction with NH_3 or organic amine to form SOA (De Haan et al., 2019; Aiona et al., 2017; Li et al., 2021b; Yasmeen et al., 2010; Zhang et al., 2022). Currently, the SOA module in chemical transport models primarily encompasses the homogeneous reactions of various volatility VOCs and heterogeneous reactions of isoprene epoxydiol, glyoxal, methylglyoxal, hydroxymethyl-methyl- α -lactone, 2-methylglyceric acid, and 2-methyltetrols on the aerosol surface. Notably, these models do not account for SOA formation from the heterogeneous photochemical reactions of acetone on aerosols (Fu et al., 2008; L. Huang et al., 2024; Q. Huang et al., 2024; He et al., 2024; Zheng et al., 2023). However, Ge et al. (2017) found that other products derived from acetone photo-oxidation such as alcohols and organic acids can also dissolve into the aqueous phase and transform into SOA by esterification, indicating that only considering the uptake of MGly will probably underestimate the contribution of acetone to the global SOA production. Thus, it is necessary to investigate the SOA formation from acetone and compare it with MGly-SOA.

In this work, we quantitatively investigated the effects of deliquescent seeds and NH_3 on SOA formation from the photochemical reaction of acetone via chamber experiments, and compared the difference of SOA formation processes in the presence of different seed particles. For the first time we revealed a key role of seed acidity in controlling the yield and formation pathways of SOA from acetone photochemical reactions, in which NH_3 and dust particles can greatly enhance the production and light absorption of acetone-derived SOA.

2 Experiment section

2.1 Materials and methods

All batch-mode experiments in this study were performed in a 4 m³ sealed Teflon smog chamber (Fig. S1 in the Supplement). Firstly, zero air and seed particles were introduced into the chamber. Then, acetone, H_2O_2 , and NH_3 were introduced sequentially for the heterogeneous reactions. The experiment details are reported by our previous studies (Ge et al., 2019; Zhang et al., 2021; S. Liu et al., 2021).

Briefly, zero air produced by the Zero Air Supply (Model 111 and Model 1150, Thermo Scientific, USA) was

used as the background gas in this study. Saturated water vapor flow produced by bubbling zero air through ultrapure water (Milli Q, 18.2 M Ω , Millipore Ltd., USA) was introduced into the chamber for adjusting the relative humidity (85 ± 1.0 % RH). Three types of water solutions containing Na₂SO₄, (NH₄)₂SO₄, and NH₄HSO₄ were nebulized to produce seed particles. A polydisperse mode of wetted inorganic aerosols was generated from the solutions using a single jet atomizer (7388SJA, TSI) and directly introduced into the chamber as droplets without any desiccation. Reactant gases including acetone, H₂O₂, NH₃, and SO₂ were added separately into the chamber along with a N₂ flow using a glass syringe (Liu et al., 2022; S. J. Liu et al., 2021).

2.2 Smog chamber experiments and characterization

2.2.1 Smog chamber experiments

In this study, the chamber experiments can be divided into two phases:

- *Phase I.* SOA formation from the photochemical oxidation and photolysis of acetone on aerosols was investigated, in which the OH radicals were produced from the photolysis of H₂O₂ under 254 nm UV irradiating conditions.
- *Phase II.* The effect of NH₃ on SOA formation was explored under dark conditions.

The H₂O₂ concentrations injected into the chamber were 2.95×10^{13} molec. cm⁻³ in all experiments. The influence of different inorganic particles on the two phases was studied. To compare the influence of different inorganic particles on the SOA formation, SO₂ was added into the chamber after Phase II to produce (NH₄)₂SO₄ aerosols during the Na₂SO₄ seed experiments. All the experiments were conducted under 85 ± 1.0 % RH conditions, and thus all the seeds in the chamber were deliquescent. At the end of each experiment, aerosols in the chamber were collected on 47 mm quartz filters and stored at -20 °C prior to analysis. The experimental conditions are shown in Table S1 in the Supplement.

2.2.2 Online monitoring

RH and temperature inside the chamber were monitored online. The temperature in the chamber was stabilized at 25 ± 1 °C using air conditioners. Concentrations of VOCs and SO₂ in the chamber were monitored by a proton-transfer-reaction time-of-flight mass spectrometer (PTR-TOF-MS, Ionicon Analytik, Innsbruck, Austria) and a SO₂ analyzer (Model 43i, Thermo scientific), respectively. Size distribution and mass concentration of aerosols during the reaction process were measured by a scanning mobility particle sizer (SMPS; model 3082, USA). The real-time chemical composition evolution of aerosols in the chamber was measured

by a high-resolution time-of-flight aerosol mass spectrometer (HR-ToF-AMS; Aerodyne Research Ltd, USA), which was operated in high-sensitivity V mode with a 30 s time resolution. Prior to the experiments, ionization efficiency of the AMS was calibrated using 300 nm NH₄NO₃ particles, and the value was 5.01×10^{-8} , and the relative ionization efficiency (RIE) for ammonium was 4.6. The RIE for sulfate was calibrated using (NH₄)₂SO₄ particles, and the value was 0.8.

Particle wall loss in the chamber was corrected using a total-mass-concentration-based method, and the detailed descriptions are shown in Sect. S1 in the Supplement (Liu and Abbatt, 2021; Zhang et al., 2024). The wall loss of NH₃ and VOCs in the chamber was also corrected (see the details in Sects. S2 and S3) (Li et al., 2021a; Huang et al., 2018; X. Zhang et al., 2015). Aerosol liquid water content (ALWC) was estimated using the Extended Aerosol Inorganics Model (E-AIM) IV, and the pH values of aerosols were calculated by Eq. (1).

$$\text{pH} = -\log_{10}(\gamma_{\text{H}^+} m_{\text{H}^+}), \quad (1)$$

where γ_{H^+} and m_{H^+} were the activity coefficient and molality of H⁺ calculated by the E-AIM, respectively.

2.2.3 Offline analysis of particles

The collected samples were extracted with 15 mL of Milli-Q pure water in an ultrasonic bath for 30 min and filtered by a 0.45 μm PES syringe filter. The concentration of water-soluble organic carbon (WSOC) and the light absorption of the extracts were analyzed by a total organic carbon analyzer (model TOC/TN-LCPH, Shimadzu Inc. Japan) and a liquid waveguide capillary cell (model LWCC3000, Ocean Insight, USA) coupled with a UV-Vis spectrophotometer (ocean insight) over a wavelength range of 200–900 nm, respectively. Light absorption (Abs_{λ}) and the mass absorption coefficient (MAC) of the water extracts were calculated (see details in Sect. S4). In addition, the collected particles were extracted with pure methanol and analyzed for their chemical compositions using an ultrahigh-resolution Orbitrap mass spectrometer (Q-Exactive Orbitrap mass spectrometer, Thermo Scientific, Germany) (Jia et al., 2023). Specifically, imidazole compounds (IMs) were determined using the Orbitrap mass spectrometer, and detailed analysis methods were reported in our previous study (Liu et al., 2023).

2.2.4 Observation-based chemical box model

In this work, an observation-based model (OBM) incorporating the latest version 3.3.1 of the Master Chemical Mechanism (MCM v3.3.1; available at <http://mcm.leeds.ac.uk/MCM/>, last access: 10 September 2024; hereafter referred to as OBM-MCM) was utilized to simulate the acetone photochemical reactions in the chamber. The observation levels of

acetone, acetaldehyde, formic acid and acetic acid throughout the photochemical reactions, along with meteorological parameters (temperature and relative humidity) and the initial H_2O_2 concentration, were incorporated into the OBM-MCM as constraints. The comprehensive MCM mechanisms related to the photochemical reactions of acetone and other VOCs observed in this work were also incorporated into the OBM-MCM. The photolysis rate for H_2O_2 is $9.1 \times 10^{-6} \text{ s}^{-1}$. The average concentration of OH radicals during the reactions is $5.89 \times 10^6 \text{ molec. cm}^{-3}$. The time series of OH and HO_2 radical concentrations are shown in Fig. S2.

3 Results and discussion

3.1 Formation of acetone-derived SOA

Figure 1 shows the time evolution of gas- and particle-phase species during the reaction in the presence of $(\text{NH}_4)_2\text{SO}_4$ seeds. In this study the whole smog chamber reaction process consists of two phases, of which Phase I is a photochemical reaction of acetone without $\text{NH}_3(\text{g})$, and Phase II is a dark reaction with introduced NH_3 . During Phase I, once the light was turned on, the gas-phase concentrations of MGly, acetaldehyde, formic acid, and acetic acid quickly increased with decreasing acetone (Phase I, Fig. 1a), while SOAs were instantly produced and sharply increased to over $90 \mu\text{g m}^{-3}$ (Phase I, Fig. 1b). When the concentration of SOA during Phase I did not change and even started to decrease, the light was turned off, and $\text{NH}_3(\text{g})$ was introduced into the chamber (Phase II). According to the formation time of these gas products, acetaldehyde and MGly are often considered the first-generation products, while formic and acetic acids are usually considered the final-generation products (Poulain et al., 2010). The oxidation state of compounds (OSc) and O/C elemental ratio of SOA in the aerosol phase continuously increased during the reaction process (Fig. 1c), which corresponds to a decreasing fraction of CHO^+ plus $\text{C}_2\text{H}_3\text{O}^+$ and an increasing fraction of CO_2^+ (Fig. 1d), indicating an efficient conversion of carbonyl compounds to carboxylic acid compounds. In Phase I, we observed an aerosol-phase decreasing trend of molar ratio of NH_4^+ to SO_4^{2-} , which was accompanied by an increasing trend of the N/C ratio of SOA (Fig. 1b and c), indicating a transformation of inorganic NH_4^+ to N-containing organic compounds. Such a phenomenon can be ascribed to the uptake of organic acid products and a reaction of carbonyl compounds with the $(\text{NH}_4)_2\text{SO}_4$ seeds during Phase I (Liu et al., 2023; Li et al., 2021b). The pH value of particles reduced rapidly from the initial 4.89 to 1.77 after a 30 min reaction due to the formation of NH_4HSO_4 . The increased acidity can hinder the gas–particle partitioning of gas-phase reaction products such as formic acid, acetic acid, and methylglyoxal (Lv et al., 2022; Zhao et al., 2006), as most weak acids are unable to dissociate at $\text{pH} < 2$ (Tilgner et al., 2021). Therefore, SOA formation by the partitioning process sharply decreased af-

ter the 30 min reaction time, resulting in a slow increase in the SOA concentration. Subsequently, the SOA is primarily formed through aqueous reactions on aerosols, leading to a persistent increase in the O/C ratio, N/C ratio, and oxidation state of SOA.

As shown in Fig. 1a and b, after NH_3 was introduced (Phase II), the formic and acetic acids decreased dramatically, while SOA did not change obviously, suggesting that the decreases of the gas acids were mainly resulted from the enhanced wall loss due to the neutralization of NH_3 on the chamber wall. Interestingly, we found that during the dark reaction, OSc and the O/C ratio of SOA decreased slightly, but their N/C ratio increased significantly by a factor of approximately 2 (Fig. 1c), implying that chemical composition of SOA changed remarkably after NH_3 was introduced, although the SOA mass did not change evidently (Fig. 1c, Phase II). Moreover, such a slight decrement of O/C and a significant increment of N/C in the elemental compositions of SOA (Fig. 1c) were also accompanied by a sharp increase in CHN family fragment fractions (Fig. 1d, Phase II), which can be explained by carbonyl–ammonium condensation under the dark conditions that forms a C–N bond and loses a H_2O molecule (Aiona et al., 2017; Li et al., 2021b; Liu et al., 2023). Such an aqueous-phase dark reaction after NH_3 was introduced can be further revealed by a change in SOA composition during Phase II, which is characterized by higher fractions of $\text{C}_x\text{H}_y\text{N}_1$ fragments in Phase II than those in Phase I (Fig. 2). Organic ammonium salt would contribute NH_x fragments instead of fragments containing N, C, and O elements. Therefore, the CHN species should be generated from the reactions of carbonyls with NH_3 rather than the acid–base neutralization of organic acid with NH_3 (Liu et al., 2015). As seen in Fig. S3, the CHN family species mainly include CHN, CH_4N , $\text{C}_2\text{H}_6\text{N}$, $\text{C}_2\text{H}_7\text{N}$, $\text{C}_2\text{H}_4\text{N}$, CH_5N , and $\text{C}_3\text{H}_6\text{N}$ ions, which are similar to the fragments of N-containing organics produced from the reaction of carbonyls with $(\text{NH}_4)_2\text{SO}_4$ (De Haan et al., 2010) and increased significantly during Phase II, resulting in an enhancing role of NH_3 in the SOA formation from acetone photochemical reaction.

3.2 Enhancing effect of seeds on the SOA formation

As shown in Fig. S4, the concentration of SOA derived from acetone photochemical reactions in the presence of $(\text{NH}_4)_2\text{SO}_4$ seeds is 20 times higher than that in the absence of the seeds, suggesting that the occurrence of $(\text{NH}_4)_2\text{SO}_4$ seeds remarkably promoted the SOA formation. Such an enhancing role was also found for Na_2SO_4 and NH_4HSO_4 seeds (Fig. S5). Because of the significant influence of surface area of aerosols on the multiphase reactions (Huang et al., 2016), the SOA formation amounts were normalized by the aerosol surface area (SA) to eliminate the interference of the difference in seed concentrations. As seen in Fig. 3a, the normalized concentration of SOA on Na_2SO_4 seeds is 2

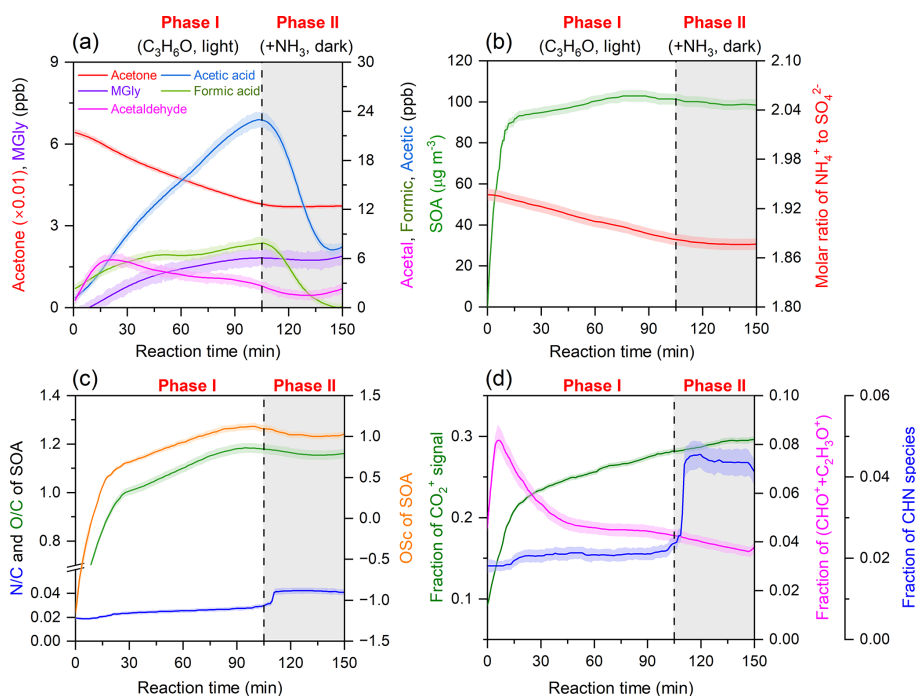


Figure 1. Time evolution of gas-phase and aerosol-phase species in the presence of $(\text{NH}_4)_2\text{SO}_4$ seeds during the acetone oxidation process (Phase I, photochemical reactions of acetone by OH radicals without NH_3 , and Phase II, reaction of acetone oxidation products with NH_3 under dark conditions). (a) Gas-phase compounds; (b) SOA and molar ratio of NH_4^+ to SO_4^{2-} in the aerosol-phase; (c) N/C and O/C elemental ratios and oxidation state of compounds ($\text{OSc} = 2 \times \text{O/C} - \text{H/C}$) of SOA; (d) relative abundances of CO_2^+ , the sum of CHO^+ plus $\text{C}_2\text{H}_3\text{O}^+$, and CHN family fragments of SOA.

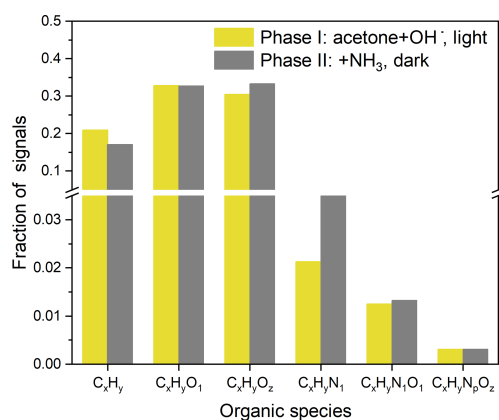


Figure 2. Fragment compositions of acetone-derived SOA in the presence of $(\text{NH}_4)_2\text{SO}_4$ seeds between the two reaction phases (Phase I, oxidation of acetone by OH radicals without NH_3 , and Phase II, reaction of acetone oxidation products with NH_3 under dark conditions).

times larger than that on $(\text{NH}_4)_2\text{SO}_4$ and NH_4HSO_4 seeds, respectively, indicating that the difference in physicochemical properties of seeds is of different promoting effects on the SOA formation. MGly is one of the first-generation oxidation products of the acetone photochemical reactions and

also one of the critical precursors of SOA (Li et al., 2021b). Therefore, we choose it as the target compound to explore the effect of the seeds on the SOA formation. The multi-phase reactions of acetone-derived MGly in the chamber can be divided into two processes: the gas–particle partitioning and the subsequent aqueous phase reactions (Srivastava et al., 2022; Waxman et al., 2015), which are further discussed in the following.

3.2.1 The effects on the gas-to-particle phase partitioning

It has been reported that the presence of salts in aerosol aqueous phase can significantly influence the gas–particle phase partitioning of MGly, which can decrease the solubility of MGly, i.e., a salting-out effect (Waxman et al., 2015). In this study, the effective Henry's law constants ($K_{\text{H, salt}}$) of MGly in the aqueous phase of various seeds were further estimated by Eq. (2) (Waxman et al., 2015; Cui et al., 2021).

$$\log\left(\frac{K_{\text{H,w}}}{K_{\text{H,salt}}}\right) = K_{\text{S}} c_{\text{salt}}, \quad (2)$$

where $K_{\text{H,w}}$ and $K_{\text{H, salt}}$ are the Henry's law constants of MGly in pure water ($3.71 \times 10^3 \text{ M atm}^{-1}$) (Curry et al., 2018) and in a salt solution, respectively; K_{S} is the salting constant or Setschenow constant, which is 0.16 M^{-1} , used in this work

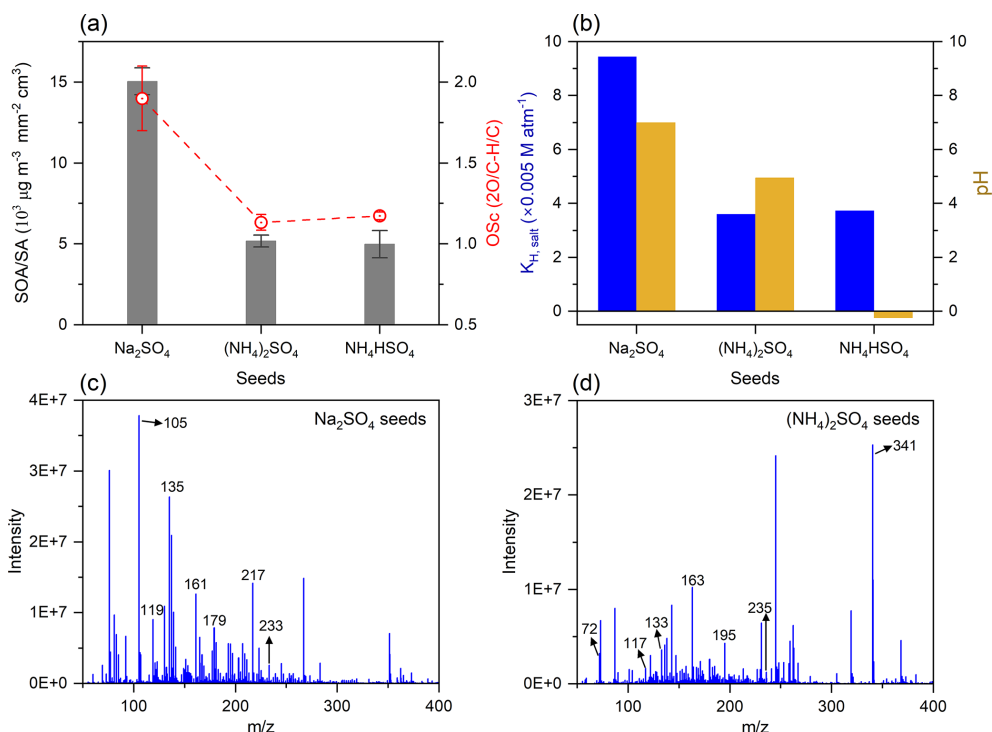


Figure 3. Effect of seed acidity on SOA formation. (a) The amount SOA normalized by the surface area (SA) of aerosols and OSc of SOA in the presence of different seeds in Phase I. (b) Effective Henry's law constants ($K_{\text{H,salt}}$) of MGly and acidity (pH) of inorganic aerosols during the reaction. (c, d) Mass spectra of SOA from acetone oxidations by OH radicals with no NH_3 in the presence of Na_2SO_4 and $(\text{NH}_4)_2\text{SO}_4$ seeds, respectively.

(Waxman et al., 2015), supposing that the K_{S} values are similar in the three types of inorganic aerosols (Gen et al., 2018); and c_{salt} is the salt concentration in molality.

As shown in Fig. 3b, $K_{\text{H,salt}}$ of MGly on Na_2SO_4 seeds in this study is more than 2 times that on $(\text{NH}_4)_2\text{SO}_4$ and NH_4HSO_4 seeds, respectively, because of its lower salt concentration and weaker salting-out effect. The acidity of the aerosol aqueous phase can also affect the uptake of MGly. For instance, Zhao et al. (2006) found that the effective Henry's law constant of MGly decreased with an increase in aqueous acidity in their laboratory experiments. As shown in Fig. 3b, the pH values of Na_2SO_4 , $(\text{NH}_4)_2\text{SO}_4$, and NH_4HSO_4 seeds in our chamber study are 7.0, 4.9, and -0.2 , respectively, indicating that the neutral nature of Na_2SO_4 seeds is more favorable for the uptake of MGly compared to the two other acidic seeds. The SOA formation with NH_4HSO_4 seeds is similar to that with $(\text{NH}_4)_2\text{SO}_4$ seeds, which is possibly caused by the promotion of residual trace NH_3 in the chamber on the uptake of acidic organics (Fig. 3a).

In addition, the higher OSc and larger fraction of $\text{C}_x\text{H}_y\text{O}_z$ signals of SOA on Na_2SO_4 seeds (Figs. 3a and S6) may also be caused by enhanced uptake of carboxylic acids (e.g., formic and acetic acids) in comparison with those by the two other kinds of acidic seeds (Huang et al., 2016), which also

resulted in the less abundant formic and acetic acids in the gas phase at the end of Phase I during the Na_2SO_4 seed experiment (Fig. S7).

3.2.2 The effects on the aqueous reaction

The aqueous formation of SOA could be affected by the phase state and acidity of aerosols (Amorim et al., 2020, 2021; Shen et al., 2022). Since particles in all the experiments of this work are deliquesced under 85% RH conditions (Wong et al., 2015; Bateman et al., 2015), the influence of the phase state can be neglected. Here, we focus on the impact of aerosol acidity on the SOA formation pathway by characterizing the chemical composition of SOA in the chamber using ESI-Q-MS technique. The mass spectra of SOA formed on different seeds are shown in Fig. 3c and d, and the detail peak assignments are presented in Table S2, respectively. As shown by Fig. 3c and d, the main peaks of SOA formed on Na_2SO_4 seeds are located in the mass range lower than $m/z = 200$, whereas the main peaks of SOA formed on $(\text{NH}_4)_2\text{SO}_4$ seeds are located in the mass range larger than $m/z = 200$, clearly showing that SOAs formed on neutral aerosols are dominantly smaller molecules, while those formed on acidic aerosols are dominantly larger molecules. The phenomenon can be attributed to the promotion of the acid-catalyzed reactions in

the formation of high-order oligomers on the acidic seeds (Jang et al., 2002; R. Zhang et al., 2015). On the other hand, such different formation pathways of SOA can also be explained by the difference of reactive oxygen species formed in the aqueous phase of the different aerosols. On neutral aerosols, organic hydroperoxides produced from the reaction of peroxides radicals and HO₂ radicals decompose and generate OH radicals through the cleavage of the weaker O–O bond (Wei et al., 2022). Then, the OH radicals oxidize the oligomers to low-molecular-weight (LMW) compounds (Zhao et al., 2017). In contrast, on acidic aerosols, the acid-catalyzed thermal decomposition of the organic hydroperoxides leads to the formation of alcohol and ketone as the end products, which does not involve radical formation (Wei et al., 2022; Yaremenko et al., 2016). Then, the carbonyls in the aqueous phase will undergo hydration, oligomerization, and acid-catalyzed aldol condensation to form high-molecular-weight (HMW) compounds (R. Zhang et al., 2015; Kenseth et al., 2023; Li et al., 2021b). Such an explanation can be supported by the higher OSc of SOA formed on the neutral aerosols (Fig. 3a). On the other hand, the lower SOA mass formed on acidic aerosols can also be attributed in part to the different reactivity of OH radical to carboxylic group; the OH radical does not react with the carboxyl group (COOH) rapidly through H abstraction from an O–H bond, but the OH radical is more reactive to the carboxylate group (ROO[−]) by abstracting an electron, which can result in a high SOA yield on neutral aerosols (Amorim et al., 2021; Herrmann et al., 2015).

3.3 The different effect of NH₃ on SOA formation on different seeds

As shown in Fig. 4a, when NH₃ was introduced into the reaction system (Phase II), the ratio of N/C of SOA increased significantly because of the reaction of NH₄⁺/NH₃ with carbonyls on acidic (NH₄)₂SO₄ and NH₄HSO₄ seeds, but such an evident change was not observed in the presence of NH₃ for neutral Na₂SO₄ seeds. One of the reasons is that NH₃ dissolves more readily on acidic aerosols. The gas-to-particle phase partition coefficients of NH₃ ($\epsilon(\text{NH}_4^+)$) on different seeds were calculated (Sect. S5) (Guo et al., 2017; Lv et al., 2023). As shown in Fig. 4b, $\epsilon(\text{NH}_4^+)$ is zero and 1.0 for Na₂SO₄ and NH₄HSO₄ seeds, respectively, suggesting that NH₃ was almost not absorbed by Na₂SO₄ seeds but efficiently absorbed by NH₄HSO₄ seeds. The phenomenon can be confirmed by Fig. S8; more N mass partitioned on more acidic aerosols. Liu et al. (2015) analyzed the uptake of NH₃ onto SOA and also found that the uptake coefficient positively correlated with particle acidity. Several studies put forward that the reaction of NH₃ with carbonyl is likely acid-catalyzed (R. Zhang et al., 2015; Liu et al., 2015). However, such a conclusion was inconsistent with the phenomenon observed by Yang et al. (2024); they found that the light absorption ability of brown carbon produced from the aque-

ous reactions of α -dicarbonyls with ammonium or amine increased exponentially with the increase in pH. To resolve such a disagreement, we analyzed the chemical composition of SOA detected by the HR-ToF-AMS in different reaction phases. As shown in Fig. S6a–d, no change was observed on Na₂SO₄ particles in Phase II after NH₃ was introduced, but the fraction of the CHN family species increased dramatically on (NH₄)₂SO₄ and NH₄HSO₄ particles in Phase II. Hence, we supposed that NH₃ can promote the formation of N-containing SOA on acidic aerosols significantly via reacting with carbonyl compounds. To verify such an assumption, we performed additional experiments by introducing 500 ppb SO₂ into the chamber in the presence of Na₂SO₄ seeds after Phase II (Phase III, Fig. S9). The addition of SO₂ resulted in (NH₄)₂SO₄ being produced immediately in the chamber (Phase III, Fig. S9a), and then the fraction of CHN species increased sharply (Phase III, Fig. S9b). Such results again demonstrate the pivotal role of acidic particles in the formation of N-containing SOA.

The optical properties of the acetone-derived SOA on different particles were measured by the LWCC. Compared with the light absorption spectra of SOA formed on Na₂SO₄ seeds in the absence of SO₂, an enhanced MAC peak at ~ 270 nm was observed for SOA formed on (NH₄)₂SO₄ seeds and on Na₂SO₄ seeds with SO₂, respectively (Fig. 4c). Such enhanced absorption is in agreement with that of the products from the MGly and (NH₄)₂SO₄ reaction, which displays prominent peaks at < 240 and ~ 270 nm, with a tail extending to > 350 nm (Kasthuriarachchi et al., 2020). The increased absorption peak at 270 nm can be ascribed to a formation of imidazoles through the reaction of MGly with NH₄⁺ (You et al., 2020). In this work, 1H-imidazole-4-carboxylic acid was observed for the SOA formed on (NH₄)₂SO₄ seeds (Fig. 4d). However, the absorption peak at ~ 270 nm for the products of the Na₂SO₄ particles in the absence of SO₂ was weaker than that with (NH₄)₂SO₄ seeds significantly (Fig. 4c), further confirming the enhancement effect of acidic particles on the formation of light-absorbing SOA, which is often termed as brown carbon.

3.4 Formation mechanisms of acetone-derived SOA on different seeds

Figure 5 shows the mass yield and MAC of acetone-derived SOA at the end of Phase II. Clearly, SOA is formed more readily on neutral Na₂SO₄ seeds than on acidic (NH₄)₂SO₄ seeds. However, in the presence of NH₃, SOAs formed on (NH₄)₂SO₄ seeds are more light-absorbing than those formed on Na₂SO₄ aerosols, suggesting that a stronger acidity of aerosol phase is favorable for the formation of light-absorbing organics because NH₃ cannot be taken up by neutral aerosols, and thus carbonyl–ammonium condensation is only active under acidic conditions and produces light-absorbing N-containing organics.

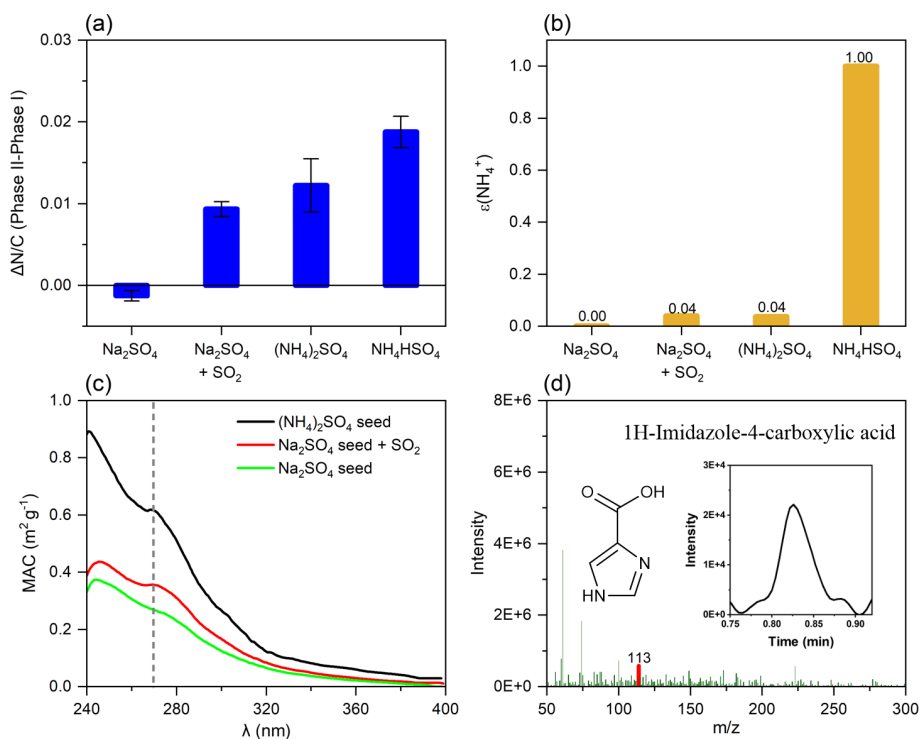


Figure 4. Effect of ammonia on SOA formation. (a) The difference in N/C ratio of Phase II relative to Phase I on different seeds. (b) Partitioning coefficients of NH_3 ($\varepsilon(\text{NH}_4^+)$) on different seeds in the chamber. (c) MAC of acetone-derived SOA in the presence of different seeds. (d) Mass spectrum of 1H-imidazole-4-carboxylic acid formed during the heterogeneous oxidation of acetone in the presence of $(\text{NH}_4)_2\text{SO}_4$ seed.

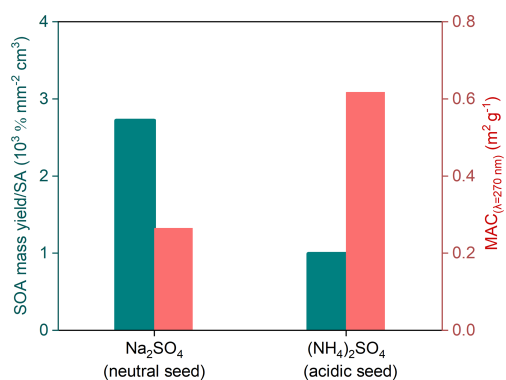


Figure 5. SOA yield (green) and $\text{MAC}_{\lambda=270 \text{ nm}}$ (red) of acetone-derived SOA in the presence of Na_2SO_4 and $(\text{NH}_4)_2\text{SO}_4$ seeds with NH_3 under dark conditions (Phase II), respectively.

By combining the gas- and aerosol-phase chemistry evolution in the chamber, a chemical mechanism for SOA formation from acetone multiphase photochemical reactions on different aerosols in the presence of NH_3 was proposed (Fig. 6). The photochemical reactions of acetone in this work include photolysis and oxidation by OH radicals. According to the results of OBM-MCM, the reaction rates of photolysis and OH oxidation are 3.66×10^6 and $1.32 \times$

$10^7 \text{ molec. cm}^{-3} \text{ s}^{-1}$, respectively. These two photochemical reactions produce various peroxy radical (RO_2) and undergo two RO_2 fates, $\text{RO}_2 + \text{HO}_2$ and $\text{RO}_2 + \text{RO}_2$ reactions. The concentrations of three main RO_2 concentrations and loss rates of two RO_2 pathways during the experiments are shown in Figs. S11 and S12, respectively. Initially, CH_3O_2 and CH_3CO_3 are predominantly formed from the photolysis of acetone, and $\text{CH}_3\text{COCH}_2\text{O}_2$ is generated from oxidation by OH radicals (Ge et al., 2017). Meanwhile, both CH_3O_2 and CH_3CO_2 can be produced within the $\text{CH}_3\text{COCH}_2\text{O}_2$ chemistry, resulting in their higher concentrations compared to $\text{CH}_3\text{COCH}_2\text{O}_2$ and a consistent increase in concentrations throughout the experiments. Obviously, $\text{RO}_2 + \text{HO}_2$ was the main pathway in RO_2 chemistry, the loss rate of which was 3.19 times that of the $\text{RO}_2 + \text{RO}_2$ pathway. Concentrations of the main gaseous products from RO_2 chemistry are shown in Table S3. $\text{C}_2\text{H}_4\text{O}_3$ and $\text{C}_3\text{H}_6\text{O}_3$ are intermediate-volatility organic compounds (IVOCs) and can undergo gas–particle partitioning readily to form SOA. Moreover, there are abundant gas-phase intermediate products containing hydrophilic functional groups such as alcohol, ketone, and organic acids formed from acetone photochemical reactions, which can dissolve into aqueous phase and undergo further oxidation reactions, esterification reactions, and radical–radical reactions to form SOA on particles (Poulain et al., 2010; Ge

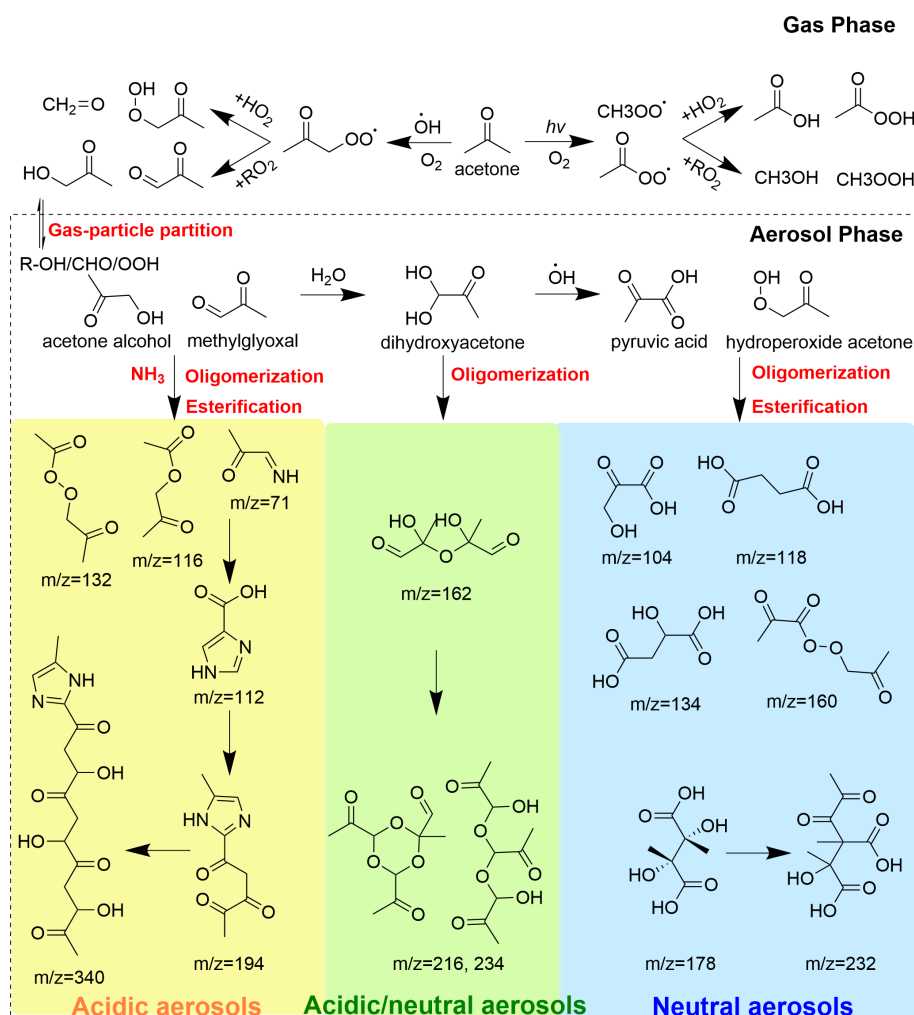


Figure 6. A diagram for the formation pathway of SOA derived from acetone oxidation in the atmosphere.

et al., 2017). For example, the dissolved MGly can be hydrolyzed and then oxidized into organic acids such as pyruvic and oxalic acids, or it proceeds to a series of oligomerization to produce many oligomers, giving rise to SOA formation. The acetone alcohol can react with acetic acid to form esters $C_5H_8O_3$ in the aqueous phase. The organic hydroperoxide $C_3H_6O_3$ produced from the acetone- RO_2+HO_2 pathway can also react with acetic acid and pyruvic acid to form $C_5H_8O_4$ and $C_6H_8O_5$ in the particle phase, respectively. These esterification reactions can also contribute to SOA formation effectively.

In the presence of NH_4^+ , carbonyl compounds in the aerosol phase can react with free NH_3 molecules and produce N-containing SOA including imine, imidazole, and other oligomers (Liu et al., 2023). LMW SOAs are formed readily in the neutral aerosol phase, while HMW SOA and N-containing brown carbon are formed favorably in the acidic aerosol phase because the acidic condition is favorable for the uptake of NH_3 . The carbenium cations, which are pro-

duced from protonation and dehydration of the hydration products of MGly under acidic conditions, are the key intermediates for formation and propagation of oligomerization (Ji et al., 2020). The oligomers and N heterocycles are produced from the nucleophilic addition of the negative hydroxyl O atom of hydration products and the negative N-atom of NH_3 to the carbenium cations, respectively (Li et al., 2021b, a).

3.5 Comparison of SOA from acetone with that from MGly in the chamber

Currently, estimations of acetone-derived SOA by models only consider its product MGly as the precursor (Fu et al., 2008). The uptake coefficient (γ) of MGly used in their work is 2.9×10^{-3} without taking into account the influence of salting effects. Curry et al. (2018) revised the γ to 10^{-10} – 10^{-6} after considering salting effects, aerosol thermodynamics, mass transfer, and irreversible reactions of or-

Table 1. Concentrations of total SOA formed in the chamber and that formed only from the uptake of methylglyoxal (MGly) in the chamber.

Seed	SOA ^a	Surface area of seeds	MGly	γ^b	SOA _{MGly} ^c	SOA/SOA _{MGly}
	($\mu\text{g m}^{-3}$)	($\text{m}^2 \text{m}^{-3}$)	($\mu\text{g m}^{-3}$)		($\mu\text{g m}^{-3}$)	
Na ₂ SO ₄	140	9.30×10^{-3}	26.74	2.6×10^{-4}	17.17	8.2
(NH ₄) ₂ SO ₄	101	1.95×10^{-2}	42.95	2.6×10^{-4}	28.88	3.5
NH ₄ HSO ₄	57	1.14×10^{-2}	38.43	2.6×10^{-4}	20.17	2.8

^a SOA values are the concentrations of SOA on different seeds observed in the experiments. ^b The values of γ are consistent with the parameters of the irreversible uptake of MGly used in CMAQ v5.3. ^c SOA_{MGly} is the estimated concentration of SOA formed from the irreversible uptake of MGly on different aerosols.

ganic species with OH in the aqueous phase. In addition, previous laboratory studies showed a large difference among the uptake coefficients of MGly, ranging from 4.0×10^{-7} to 2.4×10^{-2} (Li et al., 2023, 2021b). Salting effects and other VOCs such as formaldehyde and acetaldehyde can also influence the SOA formation from aqueous reaction of MGly (Rodriguez et al., 2017; Waxman et al., 2015). These documented values suggest a big uncertainty for SOA model work on MGly. Currently, the uptake coefficient (γ) of MGly is set as 2.6×10^{-4} in CMAQ v5.3 (Chen et al., 2021). Hence, the concentration of SOA in the chamber formed only from the irreversible uptake of MGly can be calculated by Eq. (3) (Chen et al., 2021; Li et al., 2023).

$$\frac{\partial \text{aqSOA}}{\partial t} = \left(\frac{\alpha}{D_g} + \frac{4}{v_{\text{MGly}} \gamma_{\text{MGly}}} \right)^{-1} A [\text{MGly}], \quad (3)$$

where $\frac{\partial \text{aqSOA}}{\partial t}$ is the formation rate of SOA in experiments, α is the effective radius of aerosols, D_g is the gas-phase molecular diffusion coefficient, v_{MGly} is the gas-phase mean molecular speed of MGly, A is the aerosol surface area per unit air volume, and $[\text{MGly}]$ is the vapor-wall-loss-corrected concentration of MGly (see details in Sect. S3).

As shown in Table 1, the concentration of the total SOA-derived from acetone photochemical reaction in the chamber is 2.8–8.2 times that formed only from the irreversible uptake of MGly, suggesting that only considering the role of MGly will inevitably underestimate the contribution of acetone to SOA production in a continental atmosphere, which is often characterized by high loadings of acetone and aerosols.

4 Conclusions

In this study we investigated the mass yield and formation mechanism of SOA from acetone photochemical reactions in the presence of preexisting haze particles ((NH₄)₂SO₄ and NH₄HSO₄) and saline mineral particles (Na₂SO₄) under ammonia-rich conditions. We found that the presence of seeds can significantly promote the formation of acetone-derived SOA, and the SOA yield on Na₂SO₄ seeds is larger than that on acidic (NH₄)₂SO₄ and NH₄HSO₄ seeds, indicating that the differences in physicochemical properties of

preexisting aerosols are of different promoting effects on the acetone-derived SOA formation. In comparison with those of (NH₄)₂SO₄ and NH₄HSO₄ seeds, the weaker salting-out effect and lower acidity of Na₂SO₄ seeds are in favor of the gas-to-particle partitioning of the SOA precursors. Moreover, SOAs formed on the neutral seeds are dominated by smaller molecules with a higher OSc, while those formed on the acidic seeds are dominated by larger molecules with a lower OSc.

Because NH₃ cannot be taken up by neutral aerosols, the heterogeneous reaction of carbonyl with ammonium is only active under acidic conditions, which produces light-absorbing N-containing compounds such as imidazoles, resulting in acetone-derived SOAs formed on (NH₄)₂SO₄ seeds that are more light-absorbing than those formed on Na₂SO₄ seeds. In the chamber the total SOA derived from the acetone photochemical reaction is 2.8–8.2 times that formed only from the irreversible uptake of MGly, suggesting that only considering the irreversible uptake of MGly will inevitably underestimate the contribution of acetone photochemical reactions to SOA in the atmosphere.

Data availability. Datasets are available upon request to the corresponding author, Gehui Wang (ghwang@geo.ecnu.edu.cn).

Supplement. The supplement related to this article is available online at: <https://doi.org/10.5194/acp-24-14177-2024-supplement>.

Author contributions. GW designed the experiment. SZ, XX, and LC conducted the experiments. SZ, YG, XX, LC, and GW performed the data interpretation. SZ and GW wrote the paper. CW, RL, FZ, ZL, and RL contributed to the paper with useful scientific discussions or comments.

Competing interests. The contact author has declared that none of the authors has any competing interests.

Disclaimer. Publisher's note: Copernicus Publications remains neutral with regard to jurisdictional claims made in the text, published maps, institutional affiliations, or any other geographical representation in this paper. While Copernicus Publications makes every effort to include appropriate place names, the final responsibility lies with the authors.

Acknowledgements. The authors would like to acknowledge Jianjun Li and Lijuan Li from the Institute of Earth Environment, Chinese Academy of Sciences, for their helpful discussions about the AMS results.

Financial support. This research has been supported by the National Natural Science Foundation of China (grant nos. 42130704 and U23A2030) and the National Key Research and Development Program of China (grant no. 2023YFC3707401).

Review statement. This paper was edited by Dara Salcedo and reviewed by three anonymous referees.

References

- Aiona, P. K., Lee, H. J., Leslie, R., Lin, P., Laskin, A., Laskin, J., and Nizkorodov, S. A.: Photochemistry of products of the aqueous reaction of methylglyoxal with ammonium sulfate, *ACS Earth Space Chem.*, 1, 522–532, <https://doi.org/10.1021/acsearthspacechem.7b00075>, 2017.
- Amorim, J. V., Wu, S., Klimchuk, K., Lau, C., Williams, F. J., Huang, Y., and Zhao, R.: pH dependence of the OH reactivity of organic acids in the aqueous phase, *Environ. Sci. Technol.*, 54, 12484–12492, <https://doi.org/10.1021/acs.est.0c03331>, 2020.
- Amorim, J. V., Guo, X., Gautam, T., Fang, R., Fotang, C., Williams, F. J., and Zhao, R.: Photo-oxidation of pinic acid in the aqueous phase: a mechanistic investigation under acidic and basic pH conditions, *Environ. Sci. Atmos.*, 1, 276–287, <https://doi.org/10.1039/d1ea00031d>, 2021.
- Arnold, S. R., Chipperfield, M. P., Blitz, M. A., Heard, D. E., and Pilling, M. J.: Photodissociation of acetone: Atmospheric implications of temperature-dependent quantum yields, *Geophys. Res. Lett.*, 31, L07110, <https://doi.org/10.1029/2003GL019099>, 2004.
- Bateman, A. P., Bertram, A. K., and Martin, S. T.: Hygroscopic influence on the semisolid-to-liquid transition of secondary organic materials, *J. Phys. Chem. A*, 119, 4386–4395, <https://doi.org/10.1021/jp508521c>, 2014.
- Bateman, A. P., Gong, Z., Liu, P., Sato, B., Cirino, G., Zhang, Y., Artaxo, P., Bertram, A. K., Manzi, A. O., Rizzo, L. V., Souza, R. A. F., Zaveri, R. A., and Martin, S. T.: Sub-micrometre particulate matter is primarily in liquid form over Amazon rainforest, *Nat. Geosci.*, 9, 34–37, <https://doi.org/10.1038/ngeo2599>, 2015.
- Chen, X. Y., Zhang, Y., Zhao, J., Liu, Y. M., Shen, C., Wu, L. Q., Wang, X. M., Fan, Q., Zhou, S. Z., and Hang, J.: Regional modeling of secondary organic aerosol formation over eastern China: The impact of uptake coefficients of dicarbonyls and semivolatile process of primary organic aerosol, *Sci. Total Environ.*, 793, 148176, <https://doi.org/10.1016/j.scitotenv.2021.148176>, 2021.
- Chowdhury, S., Pozzer, A., Haines, A., Klingmüller, K., Münzel, T., Paasonen, P., Sharma, A., Venkataraman, C., and Lelieveld, J.: Global health burden of ambient PM_{2.5} and the contribution of anthropogenic black carbon and organic aerosols, *Environ. Int.*, 159, 107020, <https://doi.org/10.1016/j.envint.2021.107020>, 2022.
- Cui, J. N., Sun, M., Wang, L., Guo, J., Xie, G., Zhang, J., and Zhang, R.: Gas-particle partitioning of carbonyls and its influencing factors in the urban atmosphere of Zhengzhou, China, *Sci. Total Environ.*, 751, 142027, <https://doi.org/10.1016/j.scitotenv.2020.142027>, 2021.
- Curry, L. A., Tsui, W. G., and McNeill, V. F.: Technical note: Updated parameterization of the reactive uptake of glyoxal and methylglyoxal by atmospheric aerosols and cloud droplets, *Atmos. Chem. Phys.*, 18, 9823–9830, <https://doi.org/10.5194/acp-18-9823-2018>, 2018.
- De Haan, D. O., Hawkins, L. N., Kononenko, J. A., Turley, J. J., Corrigan, A. L., Tolbert, M. A., and Jimenez, J. L.: Formation of nitrogen-containing oligomers by methylglyoxal and amines in simulated evaporating cloud droplets, *Environ. Sci. Technol.*, 45, 984–991, <https://doi.org/10.1021/es102933x>, 2010.
- De Haan, D. O., Pajunoja, A., Hawkins, L. N., Welsh, H. G., Jimenez, N. G., De Loera, A., Zauscher, M., Andretta, A. D., Joyce, B. W., De Haan, A. C., Riva, M., Cui, T. Q., Surratt, J. D., Cazaunau, M., Formenti, P., Gratién, A., Pangui, E., and Doussin, J. F.: Methylamine's Effects on Methylglyoxal-Containing Aerosol: Chemical, Physical, and Optical Changes, *ACS Earth Space Chem.*, 3, 1706–1716, <https://doi.org/10.1021/acsearthspacechem.9b00103>, 2019.
- Fu, T. M., Jacob, D. J., Wittrock, F., Burrows, J. P., Vrekoussis, M., and Henze, D. K.: Global budgets of atmospheric glyoxal and methylglyoxal, and implications for formation of secondary organic aerosols, *J. Geophys. Res.-Atmos.*, 113, D15303, <https://doi.org/10.1029/2007jd009505>, 2008.
- Ge, S., Wang, G., Zhang, S., Li, D., Xie, Y., Wu, C., Yuan, Q., Chen, J., and Zhang, H.: Abundant NH₃ in China enhances atmospheric HONO production by promoting the heterogeneous reaction of SO₂ with NO₂, *Environ. Sci. Technol.*, 53, 14339–14347, <https://doi.org/10.1021/acs.est.9b04196>, 2019.
- Ge, S. S., Xu, Y. F., and Jia, L.: Effects of inorganic seeds on secondary organic aerosol formation from photochemical oxidation of acetone in a chamber, *Atmos. Environ.*, 170, 205–215, <https://doi.org/10.1016/j.atmosenv.2017.09.036>, 2017.
- Gen, M., Huang, D. D., and Chan, C. K.: Reactive Uptake of Glyoxal by Ammonium-Containing Salt Particles as a Function of Relative Humidity, *Environ. Sci. Technol.*, 52, 6903–6911, <https://doi.org/10.1021/acs.est.8b00606>, 2018.
- Guo, H., Liu, J., Froyd, K. D., Roberts, J. M., Veres, P. R., Hayes, P. L., Jimenez, J. L., Nenes, A., and Weber, R. J.: Fine particle pH and gas-particle phase partitioning of inorganic species in Pasadena, California, during the 2010 CalNex campaign, *Atmos. Chem. Phys.*, 17, 5703–5719, <https://doi.org/10.5194/acp-17-5703-2017>, 2017.
- He, Y., Zhao, B., Wang, S., Valorso, R., Chang, X., Yin, D., Feng, B., Camredon, M., Aumont, B., Dearden, A., Jathar, S. H., Shrivastava, M., Jiang, Z., Cappa, C. D., Yee, L. D., Seinfeld, J. H., Hao, J., and Donahue, N. M.: Formation of secondary organic aerosol from wildfire emissions enhanced by long-time ageing,

- Nat. Geosci., 17, 124–129, <https://doi.org/10.1038/s41561-023-01355-4>, 2024.
- Heald, C. L., Jacob, D. J., Park, R. J., Russell, L. M., Huebert, B. J., Seinfeld, J. H., Liao, H., and Weber, R. J.: A large organic aerosol source in the free troposphere missing from current models, *Geophys. Res. Lett.*, 32, L18809, <https://doi.org/10.1029/2005GL023831>, 2005.
- Herrmann, H., Schaefer, T., Tilgner, A., Styler, S. A., Weller, C., Teich, M., and Otto, T.: Tropospheric aqueous-phase chemistry: Kinetics, mechanisms, and its coupling to a changing gas phase, *Chem. Rev.*, 115, 4259–4334, <https://doi.org/10.1021/cr500447k>, 2015.
- Huang, D. D., Zhang, X., Dalleska, N. F., Lignell, H., Coggon, M. M., Chan, C. M., Flagan, R. C., Seinfeld, J. H., and Chan, C. K.: A note on the effects of inorganic seed aerosol on the oxidation state of secondary organic aerosol- α -Pinene ozonolysis, *J. Geophys. Res.-Atmos.*, 121, 12476–12483, <https://doi.org/10.1002/2016jd025999>, 2016.
- Huang, L., Wu, Z. a., Liu, H., Yarwood, G., Huang, D., Wilson, G., Chen, H., Ji, D., Tao, J., Han, Z., Wang, Y., Wang, H., Huang, C., and Li, L.: An improved framework for efficiently modeling organic aerosol (OA) considering primary OA evaporation and secondary OA formation from VOCs, IVOCs, and SVOCs, *Environmental Science: Atmospheres*, 4, 1064–1078, <https://doi.org/10.1039/d4ea00060a>, 2024.
- Huang, Q., Lu, H., Li, J., Ying, Q., Gao, Y., Wang, H., Guo, S., Lu, K., Qin, M., and Hu, J.: Modeling the molecular composition of secondary organic aerosol under highly polluted conditions: A case study in the Yangtze River Delta Region in China, *Sci. Total Environ.*, 938, 173327, <https://doi.org/10.1016/j.scitotenv.2024.173327>, 2024.
- Huang, Y., Zhao, R., Charan, S. M., Kenseth, C. M., Zhang, X., and Seinfeld, J. H.: Unified theory of vapor–wall mass transport in Teflon-walled environmental chambers, *Environ. Sci. Technol.*, 52, 2134–2142, <https://doi.org/10.1021/acs.est.7b05575>, 2018.
- Jacob, D. J., Field, B. D., Jin, E. M., Bey, I., Li, Q., Logan, J. A., Yantosca, R. M., and Singh, H. B.: Atmospheric budget of acetone, *J. Geophys. Res.-Atmos.*, 107, ACH 5-1–ACH 5-17, <https://doi.org/10.1029/2001jd000694>, 2002.
- Jang, M., Czoschke, N. M., Lee, S., and Kamens, R. M.: Heterogeneous Atmospheric Aerosol Production by Acid-Catalyzed Particle-Phase Reactions, *Science*, 298, 814–817, <https://doi.org/10.1126/science.1075798>, 2002.
- Ji, Y. M., Shi, Q. J., Li, Y. X., An, T. C., Zheng, J., Peng, J. F., Gao, Y. P., Chen, J. Y., Li, G. Y., Wang, Y., Zhang, F., Zhang, A. L., Zhao, J. Y., Molina, M. J., and Zhang, R. Y.: Carbenium ion-mediated oligomerization of methylglyoxal for secondary organic aerosol formation, *P. Natl. Acad. Sci. USA*, 117, 13294–13299, <https://doi.org/10.1073/pnas.1912235117>, 2020.
- Jia, L., Xu, Y., and Duan, M.: Explosive formation of secondary organic aerosol due to aerosol-fog interactions, *Sci. Total Environ.*, 866, 161338, <https://doi.org/10.1016/j.scitotenv.2022.161338>, 2023.
- Jo, D. S., Nault, B. A., Tilmes, S., Gettelman, A., McCluskey, C. S., Hodzic, A., Henze, D. K., Nawaz, M. O., Fung, K. M., and Jimenez, J. L.: Global health and climate effects of organic aerosols from different sources, *Environ. Sci. Technol.*, 57, 13793–13807, <https://doi.org/10.1021/acs.est.3c02823>, 2023.
- Kampf, C. J., Waxman, E. M., Slowik, J. G., Dommen, J., Pfaffenberger, L., Praplan, A. P., Prévôt, A. S. H., Baltensperger, U., Hoffmann, T., and Volkamer, R.: Effective Henry's Law partitioning and the salting constant of glyoxal in aerosols containing sulfate, *Environ. Sci. Technol.*, 47, 4236–4244, <https://doi.org/10.1021/es400083d>, 2013.
- Kashuriarachchi, N. Y., Rivellini, L. H., Chen, X., Li, Y. J., and Lee, A. K. Y.: Effect of relative humidity on secondary brown carbon formation in aqueous droplets, *Environ. Sci. Technol.*, 54, 13207–13216, <https://doi.org/10.1021/acs.est.0c01239>, 2020.
- Kenseth, C. M., Hafeman, N. J., Rezugui, S. P., Chen, J., Huang, Y., Dalleska, N. F., Kjaergaard, H. G., Stoltz, B. M., Seinfeld, J. H., and Wennberg, P. O.: Particle-phase accretion forms dimer esters in pinene secondary organic aerosol, *Science*, 382, 787–792, <https://doi.org/10.1126/science.ad0857>, 2023.
- Li, J., Zhang, H., Li, L., Ye, F., Wang, H., Guo, S., Zhang, N., Qin, M., and Hu, J.: Modeling secondary organic aerosols in China: State of the art and perspectives, *Curr. Pollut. Rep.*, 9, 22–45, <https://doi.org/10.1007/s40726-022-00246-3>, 2023.
- Li, Y. X., Zhao, J. Y., Wang, Y., Seinfeld, J. H., and Zhang, R. Y.: Multigeneration production of secondary organic aerosol from toluene photooxidation, *Environ. Sci. Technol.*, 55, 8592–8603, <https://doi.org/10.1021/acs.est.1c02026>, 2021a.
- Li, Y. X., Ji, Y. M., Zhao, J. Y., Wang, Y., Shi, Q. J., Peng, J. F., Wang, Y. Y., Wang, C. Y., Zhang, F., Wang, Y. X., Seinfeld, J. H., and Zhang, R. Y.: Unexpected oligomerization of small alpha-dicarbonyls for secondary organic aerosol and brown carbon formation, *Environ. Sci. Technol.*, 55, 4430–4439, <https://doi.org/10.1021/acs.est.0c08066>, 2021b.
- Liu, S., Wang, Y., Xu, X., and Wang, G.: Effects of NO₂ and RH on secondary organic aerosol formation and light absorption from OH oxidation of *o*-xylene, *Chemosphere*, 308, 136541, <https://doi.org/10.1016/j.chemosphere.2022.136541>, 2022.
- Liu, S., Huang, D., Wang, Y., Zhang, S., Liu, X., Wu, C., Du, W., and Wang, G.: Synergetic effects of NH₃ and NO_x on the production and optical absorption of secondary organic aerosol formation from toluene photooxidation, *Atmos. Chem. Phys.*, 21, 17759–17773, <https://doi.org/10.5194/acp-21-17759-2021>, 2021.
- Liu, S. J., Wang, Y. Q., Wang, G. H., Zhang, S., Li, D. P., Du, L., Wu, C., Du, W., and Ge, S. S.: Enhancing effect of NO₂ on the formation of light-absorbing secondary organic aerosols from toluene photooxidation, *Sci. Total Environ.*, 794, 148714, <https://doi.org/10.1016/j.scitotenv.2021.148714>, 2021.
- Liu, T. and Abbatt, J. P. D.: Oxidation of sulfur dioxide by nitrogen dioxide accelerated at the interface of deliquesced aerosol particles, *Nat. Chem.*, 13, 1173–1177, <https://doi.org/10.1038/s41557-021-00777-0>, 2021.
- Liu, T., Huang, D. D., Li, Z., Liu, Q., Chan, M., and Chan, C. K.: Comparison of secondary organic aerosol formation from toluene on initially wet and dry ammonium sulfate particles at moderate relative humidity, *Atmos. Chem. Phys.*, 18, 5677–5689, <https://doi.org/10.5194/acp-18-5677-2018>, 2018.
- Liu, X., Wang, H., Wang, F., Lv, S., Wu, C., Zhao, Y., Zhang, S., Liu, S., Xu, X., Lei, Y., and Wang, G.: Secondary formation of atmospheric brown carbon in China haze: Implication for an enhancing role of ammonia, *Environ. Sci. Technol.*, 57, 11163–11172, <https://doi.org/10.1021/acs.est.3c03948>, 2023.

- Liu, Y., Liggio, J., Staebler, R., and Li, S.-M.: Reactive uptake of ammonia to secondary organic aerosols: kinetics of organonitrogen formation, *Atmos. Chem. Phys.*, 15, 13569–13584, <https://doi.org/10.5194/acp-15-13569-2015>, 2015.
- Lv, S., Wang, F., Wu, C., Chen, Y., Liu, S., Zhang, S., Li, D., Du, W., Zhang, F., Wang, H., Huang, C., Fu, Q., Duan, Y., and Wang, G.: Gas-to-aerosol phase partitioning of atmospheric water-soluble organic compounds at a rural site in China: An enhancing effect of NH₃ on SOA formation, *Environ. Sci. Technol.*, 56, 3915–3924, <https://doi.org/10.1021/acs.est.1c06855>, 2022.
- Lv, S., Wu, C., Wang, F., Liu, X., Zhang, S., Chen, Y., Zhang, F., Yang, Y., Wang, H., Huang, C., Fu, Q., Duan, Y., and Wang, G.: Nitrate-enhanced gas-to-particle-phase partitioning of water-soluble organic compounds in Chinese urban atmosphere: Implications for secondary organic aerosol formation, *Environ. Sci. Tech. Lett.*, 10, 14–20, <https://doi.org/10.1021/acs.estlett.2c00894>, 2023.
- Moch, J. M., Dovrou, E., Mickley, L. J., Keutsch, F. N., Liu, Z., Wang, Y., Dombek, T. L., Kuwata, M., Budisulistiorini, S. H., Yang, L., Decesari, S., Paglione, M., Alexander, B., Shao, J., Munger, J. W., and Jacob, D. J.: Global Importance of Hydroxymethanesulfonate in Ambient Particulate Matter: Implications for Air Quality, *J. Geophys. Res.-Atmos.*, 125, D032706, <https://doi.org/10.1029/2020JD032706>, 2020.
- Nguyen, T. B., Coggon, M. M., Bates, K. H., Zhang, X., Schwantes, R. H., Schilling, K. A., Loza, C. L., Flagan, R. C., Wennberg, P. O., and Seinfeld, J. H.: Organic aerosol formation from the reactive uptake of isoprene epoxydiols (IEPOX) onto non-acidified inorganic seeds, *Atmos. Chem. Phys.*, 14, 3497–3510, <https://doi.org/10.5194/acp-14-3497-2014>, 2014.
- Poulain, L., Katrib, Y., Isikli, E., Liu, Y., Wortham, H., Mirabel, P., Le Calve, S., and Monod, A.: In-cloud multiphase behaviour of acetone in the troposphere: Gas uptake, Henry's law equilibrium and aqueous phase photooxidation, *Chemosphere*, 81, 312–320, <https://doi.org/10.1016/j.chemosphere.2010.07.032>, 2010.
- Raff, J. D., Stevens, P. S., and Hites, R. A.: Relative Rate and Product Studies of the OH-Acetone Reaction, *J. Phys. Chem. A*, 109, 4728–4735, <https://doi.org/10.1021/jp0501547>, 2005.
- Riva, M., Bell, D. M., Hansen, A.-M. K., Drozd, G. T., Zhang, Z., Gold, A., Imre, D., Surratt, J. D., Glasius, M., and Zelenyuk, A.: Effect of organic coatings, humidity and aerosol acidity on multiphase chemistry of isoprene epoxydiols, *Environ. Sci. Technol.*, 50, 5580–5588, <https://doi.org/10.1021/acs.est.5b06050>, 2016.
- Riva, M., Chen, Y., Zhang, Y., Lei, Z., Olson, N. E., Boyer, H. C., Narayan, S., Yee, L. D., Green, H. S., Cui, T., Zhang, Z., Baumann, K., Fort, M., Edgerton, E., Budisulistiorini, S. H., Rose, C. A., Ribeiro, I. O., e Oliveira, R. L., dos Santos, E. O., Machado, C. M. D., Szopa, S., Zhao, Y., Alves, E. G., de Sá, S. S., Hu, W., Knipping, E. M., Shaw, S. L., Duvoisin Junior, S., de Souza, R. A. F., Palm, B. B., Jimenez, J.-L., Glasius, M., Goldstein, A. H., Pye, H. O. T., Gold, A., Turpin, B. J., Vizuete, W., Martin, S. T., Thornton, J. A., Dutcher, C. S., Ault, A. P., and Surratt, J. D.: Increasing isoprene epoxydiol-to-inorganic sulfate aerosol ratio results in extensive conversion of inorganic sulfate to organosulfur forms: Implications for aerosol physicochemical properties, *Environ. Sci. Technol.*, 53, 8682–8694, <https://doi.org/10.1021/acs.est.9b01019>, 2019.
- Rodriguez, A. A., de Loera, A., Powelson, M. H., Galloway, M. M., and Haan, D. O.: Formaldehyde and Acetaldehyde Increase Aqueous-Phase Production of Imidazoles in Methylglyoxal/Amine Mixtures: Quantifying a Secondary Organic Aerosol Formation Mechanism, *Environ. Sci. Tech. Lett.*, 4, 234–239, <https://doi.org/10.1021/acs.estlett.7b00129>, 2017.
- Seinfeld, J. H. and Pandis, S. N.: *Atmospheric Chemistry and Physics: From air pollution to climate change*, John Wiley & Sons, 2nd edn., ISBN: 978-0-471-72018-8, 2006.
- Shen, C., Zhang, W., Choczynski, J., Davies, J. F., and Zhang, H.: Phase state and relative humidity regulate the heterogeneous oxidation kinetics and pathways of organic-inorganic mixed aerosols, *Environ. Sci. Technol.*, 56, 15398–15407, <https://doi.org/10.1021/acs.est.2c04670>, 2022.
- Srivastava, D., Vu, T. V., Tong, S., Shi, Z., and Harrison, R. M.: Formation of secondary organic aerosols from anthropogenic precursors in laboratory studies, *npj Clim. Atmos. Sci.*, 5, 22, <https://doi.org/10.1038/s41612-022-00238-6>, 2022.
- Stefan, M. I. and Bolton, J. R.: Reinvestigation of the acetone degradation mechanism in dilute aqueous solution by the UV/H₂O₂ process, *Environ. Sci. Technol.*, 33, 870–873, <https://doi.org/10.1021/es9808548>, 1999.
- Tilgner, A., Schaefer, T., Alexander, B., Barth, M., Collett Jr., J. L., Fahey, K. M., Nenes, A., Pye, H. O. T., Herrmann, H., and McNeill, V. F.: Acidity and the multiphase chemistry of atmospheric aqueous particles and clouds, *Atmos. Chem. Phys.*, 21, 13483–13536, <https://doi.org/10.5194/acp-21-13483-2021>, 2021.
- Wang, C., Lei, Y. D., and Wania, F.: Effect of sodium sulfate, ammonium chloride, ammonium nitrate, and salt mixtures on aqueous phase partitioning of organic compounds, *Environ. Sci. Technol.*, 50, 12742–12749, <https://doi.org/10.1021/acs.est.6b03525>, 2016a.
- Wang, F., Lv, S., Liu, X., Lei, Y., Wu, C., Chen, Y., Zhang, F., and Wang, G.: Investigation into the differences and relationships between gasSOA and aqSOA in winter haze pollution on Chongming Island, Shanghai, based on VOCs observation, *Environ. Pollut.*, 316, 120684, <https://doi.org/10.1016/j.envpol.2022.120684>, 2023.
- Wang, G., Zhang, R., Gomez, M. E., Yang, L., Levy Zamora, M., Hu, M., Lin, Y., Peng, J., Guo, S., Meng, J., Li, J., Cheng, C., Hu, T., Ren, Y., Wang, Y., Gao, J., Cao, J., An, Z., Zhou, W., Li, G., Wang, J., Tian, P., Marrero-Ortiz, W., Secrest, J., Du, Z., Zheng, J., Shang, D., Zeng, L., Shao, M., Wang, W., Huang, Y., Wang, Y., Zhu, Y., Li, Y., Hu, J., Pan, B., Cai, L., Cheng, Y., Ji, Y., Zhang, F., Rosenfeld, D., Liss, P. S., Duce, R. A., Kolb, C. E., and Molina, M. J.: Persistent sulfate formation from London Fog to Chinese haze, *P. Natl. Acad. Sci. USA*, 113, 13630–13635, <https://doi.org/10.1073/pnas.1616540113>, 2016b.
- Wang, S., Apel, E. C., Schwantes, R. H., Bates, K. H., Jacob, D. J., Fischer, E. V., Hornbrook, R. S., Hills, A. J., Emmons, L. K., Pan, L. L., Honomichl, S., Tilmes, S., Lamarque, J.-F., Yang, M., Marandino, C. A., Saltzman, E. S., de Bruyn, W., Kameyama, S., Tanimoto, H., Omori, Y., Hall, S. R., Ullmann, K., Ryerison, T. B., Thompson, C. R., Peischl, J., Daube, B. C., Commane, R., McKain, K., Sweeney, C., Thames, A. B., Miller, D. O., Brune, W. H., Diskin, G. S., DiGangi, J. P., and Wofsy, S. C.: Global atmospheric budget of acetone: Air-sea exchange and the contribution to hydroxyl radicals, *J. Geophys. Res.-Atmos.*, 125, e2020JD032553, <https://doi.org/10.1029/2020jd032553>, 2020.
- Wang, Y., Cui, S., Fu, X., Zhang, Y., Wang, J., Fu, P., Ge, X., Li, H., and Wang, X.: Secondary organic aerosol for-

- mation from photooxidation of C₃H₆ under the presence of NH₃: Effects of seed particles, *Environ. Res.*, 211, 113064, <https://doi.org/10.1016/j.envres.2022.113064>, 2022.
- Waxman, E. M., Elm, J., Kurtén, T., Mikkelsen, K. V., Ziemann, P. J., and Volkamer, R.: Glyoxal and methylglyoxal setschenow salting constants in sulfate, nitrate, and chloride solutions: Measurements and gibbs energies, *Environ. Sci. Technol.*, 49, 11500–11508, <https://doi.org/10.1021/acs.est.5b02782>, 2015.
- Wei, J., Fang, T., and Shiraiwa, M.: Effects of acidity on reactive oxygen species formation from secondary organic aerosols, *ACS Environ. Au*, 2, 336–345, <https://doi.org/10.1021/acsenvironau.2c00018>, 2022.
- Wong, J. P. S., Lee, A. K. Y., and Abbatt, J. P. D.: Impacts of sulfate seed acidity and water content on isoprene secondary organic aerosol formation, *Environ. Sci. Technol.*, 49, 13215–13221, <https://doi.org/10.1021/acs.est.5b02686>, 2015.
- Yang, L., Huang, R.-J., Yuan, W., Huang, D. D., and Huang, C.: pH-dependent aqueous-phase brown carbon formation: Rate constants and implications for solar absorption and atmospheric photochemistry, *Environ. Sci. Technol.*, 58, 1236–1243, <https://doi.org/10.1021/acs.est.3c07631>, 2024.
- Yaremenko, I. A., Vil', V. A., Demchuk, D. V., and Terent'ev, A. O.: Rearrangements of organic peroxides and related processes, *Beilstein J. Org. Chem.*, 12, 1647–1748, <https://doi.org/10.3762/bjoc.12.162>, 2016.
- Yasmeen, F., Sauret, N., Gal, J.-F., Maria, P.-C., Massi, L., Maenhaut, W., and Claeys, M.: Characterization of oligomers from methylglyoxal under dark conditions: a pathway to produce secondary organic aerosol through cloud processing during nighttime, *Atmos. Chem. Phys.*, 10, 3803–3812, <https://doi.org/10.5194/acp-10-3803-2010>, 2010.
- You, B., Li, S. Y., Tsona, N. T., Li, J. L., Xu, L., Yang, Z. M., Cheng, S. M., Chen, Q. C., George, C., Ge, M. F., and Du, L.: Environmental processing of short-chain fatty alcohols induced by photosensitized chemistry of brown carbons, *ACS Earth Space Chem.*, 4, 631–640, <https://doi.org/10.1021/acsearthspacechem.0c00023>, 2020.
- Zhang, J., Shrivastava, M., Zelenyuk, A., Zaveri, R. A., Surratt, J. D., Riva, M., Bell, D., and Glasius, M.: Observationally constrained modeling of the reactive uptake of isoprene-derived epoxydiols under elevated relative humidity and varying acidity of seed aerosol conditions, *ACS Earth Space Chem.*, 7, 788–799, <https://doi.org/10.1021/acsearthspacechem.2c00358>, 2023.
- Zhang, R., Wang, G., Guo, S., Zamora, M. L., Ying, Q., Lin, Y., Wang, W., Hu, M., and Wang, Y.: Formation of urban fine particulate matter, *Chem. Rev.*, 115, 3803–3855, <https://doi.org/10.1021/acs.chemrev.5b00067>, 2015.
- Zhang, S., Li, D., Ge, S., Liu, S., Wu, C., Wang, Y., Chen, Y., Lv, S., Wang, F., Meng, J., and Wang, G.: Rapid sulfate formation from synergetic oxidation of SO₂ by O₃ and NO₂ under ammonia-rich conditions: Implications for the explosive growth of atmospheric PM_{2.5} during haze events in China, *Sci. Total Environ.*, 772, 144897, <https://doi.org/10.1016/j.scitotenv.2020.144897>, 2021.
- Zhang, S., Li, D., Ge, S., Wu, C., Xu, X., Liu, X., Li, R., Zhang, F., and Wang, G.: Elucidating the mechanism on the transition-metal ion-synergetic-catalyzed oxidation of SO₂ with implications for sulfate formation in Beijing haze, *Environ. Sci. Technol.*, 58, 2912–2921, <https://doi.org/10.1021/acs.est.3c08411>, 2024.
- Zhang, X., Schwantes, R. H., McVay, R. C., Lignell, H., Coggon, M. M., Flagan, R. C., and Seinfeld, J. H.: Vapor wall deposition in Teflon chambers, *Atmos. Chem. Phys.*, 15, 4197–4214, <https://doi.org/10.5194/acp-15-4197-2015>, 2015.
- Zhang, Y. M., He, L., Sun, X. M., Ventura, O. N., and Herrmann, H.: Theoretical Investigation on the Oligomerization of Methylglyoxal and Glyoxal in Aqueous Atmospheric Aerosol Particles, *ACS Earth Space Chem.*, 6, 1031–1043, <https://doi.org/10.1021/acsearthspacechem.1c00422>, 2022.
- Zhao, J., Levitt, N. P., Zhang, R., and Chen, J.: Heterogeneous Reactions of methylglyoxal in acidic media: Implications for secondary organic aerosol formation, *Environ. Sci. Technol.*, 40, 7682–7687, <https://doi.org/10.1021/es060610k>, 2006.
- Zhao, R., Aljawhary, D., Lee, A. K. Y., and Abbatt, J. P. D.: Rapid aqueous-phase photooxidation of dimers in the α -pinene secondary organic aerosol, *Environ. Sci. Tech. Lett.*, 4, 205–210, <https://doi.org/10.1021/acs.estlett.7b00148>, 2017.
- Zheng, H., Chang, X., Wang, S., Li, S., Zhao, B., Dong, Z., Ding, D., Jiang, Y., Huang, G., Huang, C., An, J., Zhou, M., Qiao, L., and Xing, J.: Sources of Organic Aerosol in China from 2005 to 2019: A Modeling Analysis, *Environ. Sci. Technol.*, 57, 5957–5966, <https://doi.org/10.1021/acs.est.2c08315>, 2023.